ornl

ORNL/TM-10778

OAK RIDGE
NATIONAL
LABORATORY

MARTIN MARIETTA

Survey of the Literature on Fractals with Possible Applications to Phase Change Processes

Lisa Anne Renker
D. G. Wilson

OAK RIDGE NATIONAL LABORATORY
CENTRAL RESEARCH LIBRARY
CIRCULATION SECTION
4500N ROOM 175
LIBRARY LOAN COPY
DO NOT TRANSFER TO ANOTHER PERSON
If you wish someone else to see this report, send in name with report and the library will arrange a loan.

OPERATED BY
MARTIN MARIETTA ENERGY SYSTEMS, INC.
FOR THE UNITED STATES
DEPARTMENT OF ENERGY

Printed in the United States of America. Available from
National Technical Information Service
U.S. Department of Commerce
5285 Port Royal Road, Springfield, Virginia 22161
NTIS price codes—Printed Copy: A03; Microfiche A01

This report was prepared as an account of work sponsored by an agency of the United States Government. Neither the United States Government nor any agency thereof, nor any of their employees, makes any warranty, express or implied, or assumes any legal liability or responsibility for the accuracy, completeness, or usefulness of any information, apparatus, product, or process disclosed, or represents that its use would not infringe privately owned rights. Reference herein to any specific commercial product, process, or service by trade name, trademark, manufacturer, or otherwise, does not necessarily constitute or imply its endorsement, recommendation, or favoring by the United States Government or any agency thereof. The views and opinions of authors expressed herein do not necessarily state or reflect those of the United States Government or any agency thereof.

ORNL/TM-10778

Engineering Physics and Mathematics Division

Mathematical Sciences Section

SURVEY OF THE LITERATURE ON FRACTALS WITH POSSIBLE APPLICATIONS TO PHASE CHANGE PROCESSES

Lisa Anne Renker
Baldwin-Wallace College

D. G. Wilson

Date Published - June 1988

Research sponsored by the
Applied Mathematical Sciences Research Program
U.S. Department of Energy
Office of Energy Research

Prepared by the
Oak Ridge National Laboratory
Oak Ridge, Tennessee 37831
operated by
MARTIN MARIETTA ENERGY SYSTEMS, INC.
for the
U.S. DEPARTMENT OF ENERGY
under Contract No. DE-AC05-84OR21400

MARTIN MARIETTA ENERGY SYSTEMS LIBRARIES

3 4456 0276325 8

Table of Contents

Abstract 1

Introduction 1

Section I - Dendrites 2

Section II - Fractals 3

Section III - Dendrites, Fractals and Dense Radial Structures 9

Conclusion 14

Bibliography 15

SURVEY OF THE LITERATURE ON FRACTALS WITH POSSIBLE APPLICATIONS TO PHASE CHANGE PROCESSES

Lisa Anne Renker

Baldwin-Wallace College

D. G. Wilson

Mathematical Sciences Section
Engineering Physics and Mathematics Division
Oak Ridge National Laboratory

ABSTRACT

This paper is a partial collection of the literature on fractals and how it applies to phase change processes, specifically solidification. Fractals can be used to model the dendrites that are formed at the interface between a liquid and a solid with restrictions because either dendrites or non-dendritic fractals may be formed by diffusion limited solidification, depending on the presence of crystalline anisotropy. This anisotropy causes the tips of the structure being formed to remain stable, leading to the formation of a dendrite, rather than splitting to form a non-dendritic fractal. An additional type of structure is found when electrodeposition is used to model solidification. The formation of this dense radial structure depends on the level of the voltage and the electrolyte concentration. These structures are formed at intermediate values where the crossover from non-dendritic fractals to dendrites occurs. Non-dendritic fractals are formed at the lower values and dendrites are formed at the higher values. A comprehensive bibliography is included with this paper.

INTRODUCTION

This paper summarizes reports of some research and experiments that have been done on dendrites, fractals and dense radial structures, in particular, the application of fractals to phase change processes. The first section deals only with dendrites and discusses dendritic growth and some of the factors affecting that growth. Dendrites are tree-like structures formed at the interface between a solid and a liquid by diffusion-limited solidification. Their growth depends on anisotropy. The presence of crystalline anisotropy causes a dendrite to grow with stable tips. The shape of the dendrite formed depends on the level of anisotropy.

The second section begins with definitions of fractal and fractal dimension. Fractals can grow in nature by diffusion-limited aggregation. When a crystalline structure is isotropic, non-dendritic fractals (characterized by split tips), rather than dendrites are formed. Two methods for calculating the fractal dimension of an object are given. Then how fractals are grown in nature and several models for simulating fractal growth are discussed.

The third section includes information about dense radial structures and electrodeposition models. Electrodeposition is sometimes used to model solidification. These models show the formation of all three structures: dendrites, non-dendritic fractals, and dense radial structures. Dense radial structures occur in a

transition region between DLA formations and dendrites. The type of pattern formed depends on the values of the voltage and the electrolyte concentration. DLA patterns are formed when one or both of these values are low. Dendrites are formed when both values are high. This section also explains how the three growth structures are related.

SECTION I - DENDRITES

Dendrites are formed at the interface between a solid and a liquid when a crystalline material freezes from its supercooled melt. These structures are pine tree shaped with arms (or branches) that are parallel to specific crystallographic directions. Dendrites are formed as a result of diffusion limited solidification. As a dendrite grows the latent heat of fusion is given off and this adds to the energy of nearby atoms. This extra heat decreases the tendency for these nearby atoms to attach to the interface, resulting in the temporary halt of growth at that part of the dendrite. Once the heat dissipates, growth will begin there again. Meanwhile, growth takes place on another part of the dendrite in a direction perpendicular to that of the prior growth. This phenomenon continues so that the final dendrite consists of a primary stalk from which smaller secondary stalks have grown perpendicular to the primary stalk. Sometimes, tertiary stalks grow perpendicularly off the secondary stalk. These secondary and tertiary stalks are added as the primary stalk becomes larger and larger which leads to the pine tree pattern. These stalks have regular branch spacing and this spacing decreases for each successive order of branching. The arms of the dendrite grow in crystallographically preferred directions. These directions are the axes of a pyramid whose sides are formed by the closest possible packed planes that can form a pyramid. This describes different directions depending on the structure of the crystal. [12,78,79,82]

Most crystal structures are anisotropic, which means that the properties of most crystals are not independent of direction. It is anisotropy, specifically the anisotropy of the growth rate and its relationship to the kinetic driving force, that causes a dendrite to form. Without this anisotropy, the dendrite's direction of growth would depend entirely on thermal conditions. [12,25,64]

Given the Stefan problem (excluding surface tension and anisotropy), there exists a continuous set of parabolic shapes for the interface that are solutions to this problem. The addition of surface tension and anisotropy causes a singularity that in turn changes the problem to a nonlinear eigenvalue problem, resulting in a discrete set of needle solutions.

A recent analysis of needle solutions by Kessler and Levine [29], shows that the fastest-moving solution is stable in a moving frame of reference and is a true dendrite. For a fixed anisotropy, the growth rate is proportional to the square of the Péclet number. The Péclet number is the ratio of a length scale (which is the radius of curvature of the leading tip of a steady-state dendrite) to the diffusion length, where the diffusion length is two times the ratio of the thermal diffusivity to the dendrite's growth velocity. [65]

Several experiments have been done using succinonitrile to predict the steady-state and free growth of dendrites. These experiments were aimed at predicting the growth velocity and geometry (the geometry as it relates to tip radius and the orientation and spacing of the side branches) of a free dendrite given the supercooling of a melt [40]. For these experiments, a solid phase grew in the direction of an axis of symmetry into a uniformly supercooled liquid.

Glicksman, et al. [21] recorded their results for both dendrite growth in a long tube and free dendrite growth. For small supercoolings of the melt in the long tube, the dendrites were individual with well-defined stems and branches that grew straight up the walls of the tube. With large supercoolings, the dendrites grew up the walls as a continuous sheath of crystals with no leading tips. At the intermediate supercoolings, the growth began with the individual dendrites as in the small supercooling experiments and later changed to the spiral morphology characteristic of large supercoolings. For all three levels of

supercooling, higher growth rates were associated with a higher purity of the succinonitrile.

The results for free dendritic growth, obtained by Glicksman, et al., op cit., were another matter entirely. For small supercoolings, the growth of the dendrites depended greatly on their inclination from vertical. Dendrites that pointed downward grew faster than dendrites that pointed upward. This was thought to be caused by the transfer of heat through the motion of the particles driven by the dendrites' temperature field. The number of dendrite arms growing into the melt increased rapidly as the degree of supercooling was increased. This increase was not because of the division of arms that were freely growing, but rather because of crystallite multiplication. As time passed, the tips of individual primary dendrites diverged radially from one another. Continual branching and rebranching of the dendrites filled the volume behind the leading tips with a fine mesh of secondary and higher order arms that grew as if they were isolated dendrites. With an increase in supercooling, the fraction of the volume of liquid changed to solid increased. This increase continued as long as some of the remaining liquid was below the equilibrium freezing temperature.

Another experiment for describing dendritic growth, done by Weinberg et al. [78], concentrated on the growth of dendrites in lead. Crystalline lead has a face-centered cubic structure consisting of "dendrite rows." The primary stalk is in a horizontal plane at the bottom of the crystal, the secondary stalks are in the vertical plane, and the tertiary stalks are again in the horizontal plane. The expected pattern that the stalks would follow is that the secondary stalks decrease in length and thickness as one moves outward on the primary stalk, and the tertiary stalks are larger and thicker near the bottom of the secondary stalk. However, this was not the case. This experiment showed that the secondary stalks do not necessarily grow at equal intervals or heights, and the larger tertiary stalks are not necessarily those closest to the bottom. The secondary and tertiary stalks did follow the primary's growth progressively increasing in size. As the dendrites grew, the interface moved along covering the rows that were initially formed. At earlier times in the growth process, the dendrites were shorter and thinner and the spacing between rows was smaller than at later times. The development of the branches was related directly to the degree of supercooling; the branches did not develop fully with less supercooling (0.5° and below). Weinberg et al. concluded that the direction of a dendrite's growth is defined by the crystallographic orientation of the dendrite and is independent of the heat flow. In this experiment, the direction of growth came within 2° of the crystallographic direction. During the solidification of metal, striations appear on the top surface of the crystal. These striations are a series of bands that are parallel to the longitudinal axis of the crystal. An increase in the growth rate causes some of the striations to widen. This widening takes over some of the neighboring striations and the boundaries between striations become jagged. These jagged boundaries are parallel to and run between the dendrite rows. In this experiment, no dendrite row ever crossed a boundary. The degree of irregularity of the crystal is greater in the sections that solidify last, where the rate of growth is the greatest.

SECTION II - FRACTALS

The word "fractal" is derived from the Latin word "*fractus*", meaning irregular and fragmented. [45] Most fractal sets have the characteristic of being self-similar; that is, each part of the shape is geometrically similar to the whole. Inherent in the definition of self-similar is the property of scaling invariance which means that it is impossible to tell what length scale was used to obtain any particular view of the shape. These two properties do not continue into infinity in the natural world as they do in mathematical fractals. The maximum size range in which natural fractals have this self-similar property is usually reached at magnifications of about four orders of magnitude. [37,62]

A fractal is sometimes defined or explained by its self-similarity property, but this is not a good definition because recently non-self-similar fractals have been discovered. [36] The definition proposed by Benoit Mandelbrot [45] is as follows: a fractal is a set for which the Hausdorff Besicovitch dimension

strictly exceeds the topological dimension. We will use the standard notation of D for the Hausdorff dimension and d_t for the topological dimension. So the definition states that for a fractal set $d_t < D$. (The topological dimension of an object is at least zero and at most equal to the Euclidean dimension of the space in which it is embedded. It is always an integer. The topological dimension for a point is zero, for a line it is one, and for a surface it is two. [35])

Every fractal has a fractal dimension. This is the same as the Hausdorff dimension used in the definition of a fractal stated above. The fractal dimension is usually not an integer. The fractal dimension quantifies the degree to which the shape fills the Euclidean space in which the object is embedded and illustrates the shape's roughness. The more compact a fractal set is, the greater the fractal dimension it has, and as the fractal dimension increases, so does the object's roughness. However, the fractal dimension of an object is never greater than the Euclidean dimension of the space in which it is contained. Therefore the fractal dimension is always greater than (by the above definition) the topological dimension and always less than or equal to the Euclidean dimension of the space. It is possible for the fractal dimension of an object to equal its Euclidean dimension, but if this occurs, then the object is not considered to be a fractal; it is considered a Euclidean set. [36,37,45]

There are at least two methods for determining the fractal dimension of an object. One method is explained by Len Sander. [68] This method determines the fractal dimension of an object by determining the average number, N, of fundamental units of repetition found within a sphere centered somewhere on the object as a function of the radius, r, of the sphere. By Euclidean geometry, the number, N, is equal to a constant, C, times the radius raised to the value of the dimension, D ($N = Cr^D$). For a line segment (see figure 1a), increasing the radius of a sphere by three triples the number of units enclosed in the sphere. This gives a dimension of one (D = log 3/log 3). For a two-dimensional figure (see figure 1b), tripling the radius increases the number of units contained within the sphere by nine (D = log 9/log 3). Given the fractal of figure 1c, tripling the radius of the sphere used increases the number of units by five and thus D = log 5/log 3 = 1.46.

Another method is explained by Richard Voss. [76] A line segment can be divided into M smaller pieces. Each of these pieces is a copy of the original line segment and each part is scaled down by a ratio of $r = 1/M$ from the whole. For a two-dimensional object, the ratio would become $r = 1/M^{1/2}$ The pattern would continue with the M on the right side of the equation raised to the reciprocal of the dimension of space. Therefore, a D-dimensional self-similar object can be divided into M smaller copies of itself with each copy scaled down by a factor of r where $M = 1/r^D$. This implies that an object's fractal dimension is D = (log M)/(log 1/r). An example of this method, using the Koch snowflake curve is shown in figure 2. This curve begins with an equilateral triangle and is generated by placing another smaller equilateral triangle on the center third of each edge of the original triangle. This process is continued on to infinity. Here, the ratio by which each copy is scaled down is 1/3. The perimeter of the object is multiplied by 4 at each stage of the construction. This gives the dimension of the snowflake to be D = log 4/log 3 = 1.26.

Fractals are thought to grow in nature by diffusion-limited aggregation (DLA). The fundamental model of this growth, proposed by Len Sander [68], is as follows. Aggregation is the adding of one particle at a time to a cluster. This particle will stick at its first contact with the growing object. Because the particle stays in the first place it contacts, the object grows in non-equilibrium. DLA starts with a smooth surface that develops bumps because of noise. The particles are then more likely to come to rest on the bumps, causing the bumps to grow faster than the holes. This effect, called screening, leads to an open structure because each particle has a higher probability of sticking near the tip than near the side. This leads to a greater instability in the system, and the growth and splitting of the tips cause a non-dendritic fractal. In the natural world, however, it is possible that particles will bounce off the first time they hit, rather than sticking right away. This will cause thicker branches, but the fractal dimension will remain the same. The random DLA model of Witten and Sander [80,81] gives a fractal dimension of 1.66 for a two-dimensional structure and a fractal dimension of 2.5 for a structure embedded in three dimensions. For two dimensions,

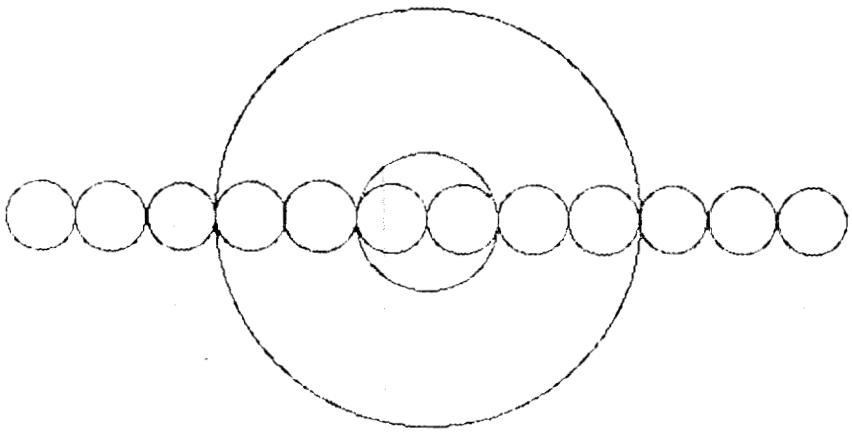

Figure 1a: A line segment has a dimension of 1.0.

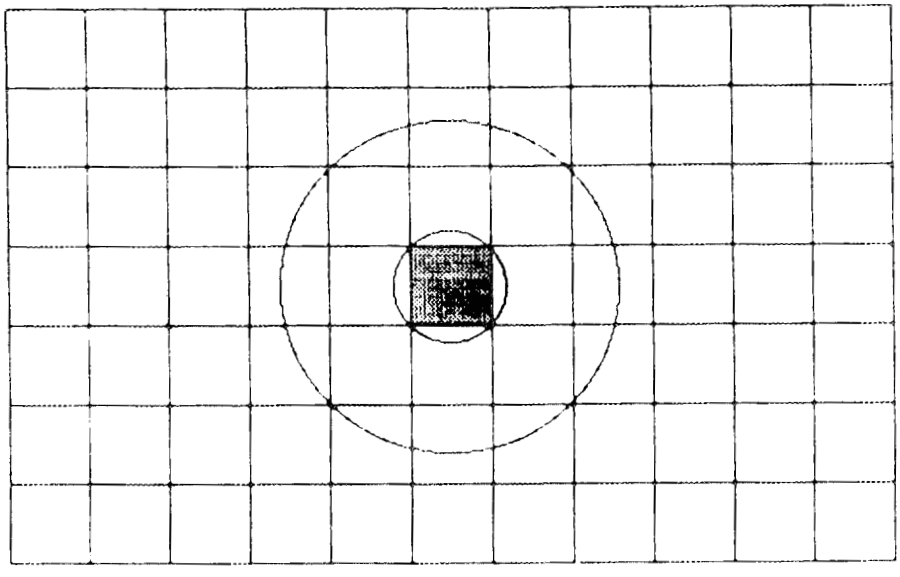

Figure 1b: This figure has a dimension of 2.0.

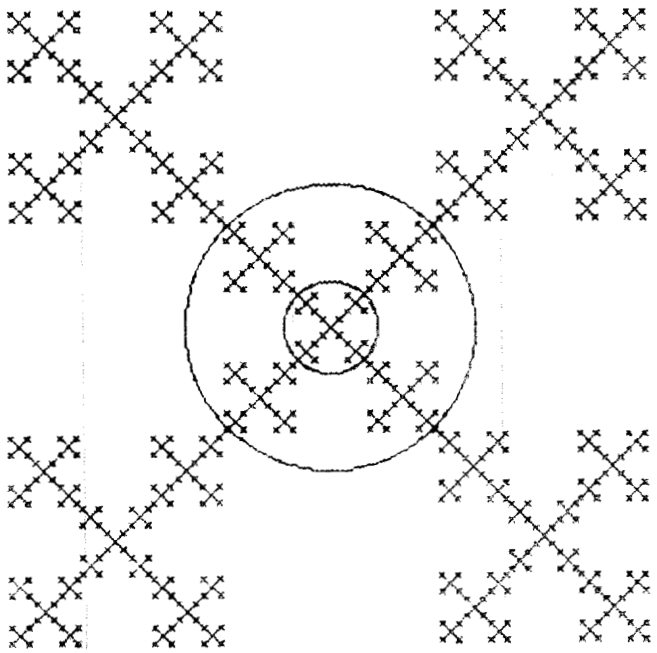

Figure 1c: This fractal has a fractal dimension of 1.46.

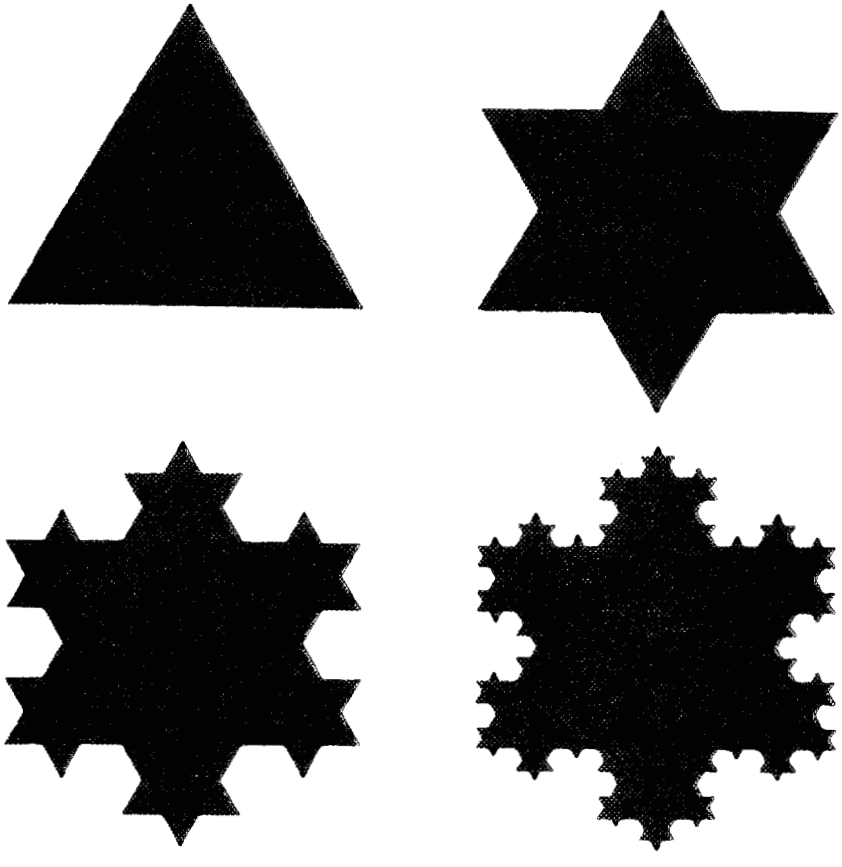

Figure 2: The Koch snowflake has a fractal dimension of 1.26.

the fractal dimension of Witten and Sander's DLA model is different from that of other random structures. Some examples of other random structures are percolation clusters and self-avoiding random walks. The fractal dimension of percolation clusters is about 1.9 and the fractal dimension of self-avoiding random walks is about 1.33. [50]

For a scale-invariant fractal, $N \sim R^D$, where N is the number of particles or subunits in a radius R of a point on the object and D is the fractal dimension of the object. If we take R to be the radius of gyration then this equation relates mass to size during the object's growth. If a fractal is scale-invariant, then all the characterization sizes are proportional. [66]

The Witten and Sander model of random particles that walk one at a time is used to represent DLA. If an object in this case is to be a fractal, it must have holes that are proportional to the size of the object itself. These holes arise because of the screening effect; particles cannot enter the interior because the arms that are already extended block the way. [66] For a two-dimensional simulation, the Witten and Sander model of DLA [80,81] has a density-density correlation function $C(r) = N^{-1}\sum\rho(r')\rho(r + r')$ where ρ is the density and r is the position of a particle. From this comes $C(r) \sim r^{-\alpha}$ for r a distance greater than a few lattice spacings but less than the size of the cluster. This is consistent with a fractal dimensionality, D, of $d_E - \alpha$ where d_E is the cluster's Euclidean dimension. The fractal dimension can also be found using the radius of gyration, R_g. We have $R_g \sim N^\beta$, for sufficiently large N, where N is the number of particles in the cluster. (R_g has a power-law dependence on N.) The fractal dimension of the cluster is $D_\beta = 1/\beta$.

Meakin [50] has proposed a model in which clusters are picked randomly and then moved by one lattice spacing. Each cluster is moved by a probability that is proportional to its mobility. When a cluster encounters another cluster, they stick together. As the clusters merge, they become larger and larger until only one cluster remains. Here, the lower cutoff length is a few lattice units and the upper length is determined by the average particle density (ρ). In Meakin's modified version of Witten and Sander's DLA model, a crossover from a fractal structure to a structure with uniform density occurs. This has a crossover length l given by $C_0\, l^{-\alpha} \approx (\rho)$ or $l \approx [(\rho)/C_0]^{-1/\alpha}$ where $C_0 \approx 1.0$ and α is $d_E - D$ (ie., α is the Hausdorff codimension). Whereas if $(\rho) \rightarrow 0$ and $l \rightarrow \infty$, the structures formed are fractal on all length scales.

Kolb et al. [33] showed that the structures formed by cluster aggregation, as well as those formed by particle aggregation, are fractal. In their particle aggregation model, N_0 particles are placed in a volume V_0. The concentration $\rho_0 = N_0/V_0$ is chosen so that the average distance between particles is larger than their radius. The particles move independently and randomly and a strong attraction causes permanent sticking. This process continues until one structure is formed. The structures were found to become less dense as they increased in size. The structures were fractal if $R_g(m) \sim m^{1/D}$ as $m \rightarrow \infty$ where D is the fractal dimensionality of the structure, R_g is the radius of gyration and m is the number of particles. The object could also be fractal if the density-density correlation function $C(r) \sim r^{-(d_E-D)}$ for $1 \ll r \ll R_g$ with $D < d_E$. D is determined by the slope of a log R_g vs. log m plot, and in two dimensions is 1.43 ± 0.03. In the cluster aggregation model of Kolb et al., there exists an upper critical dimension, above which the clusters freely interpenetrate and the fractal dimension becomes independent of the spatial dimension d_E.

SECTION III - DENDRITES, FRACTALS AND DENSE RADIAL STRUCTURES

In recent years, much interest has been given to diffusion-limited processes because DLA leads to the formation of structures that have some of the characteristics of fractals. The patterns that sometimes occur are open, random, chainlike structures that have no natural length scale, and therefore are scale invariant. [47] This observation led researchers to believe that perhaps these new patterns were fractals, and that somehow fractals and dendrites might be closely related. Many experiments have been and are being done, all with similar results; diffusion-limited aggregation leads to the formation of three different patterns of

growth: non-dendritic fractals, dendritic crystals, and dense radial structures. (See figure 3, reproduced from [67] with permission of the author.) If the system is always near equilibrium, then the internal structure and the external shape can be described with ordinary equilibrium considerations as a single crystal. As the system is moved away from equilibrium, dendritic shapes appear. These patterns result from the new length scales associated with steady-state growth. As the system moves even farther from equilibrium, disorderly growth occurs with no length scales at all. This growth is amorphous as well as scale-invariant. The most recent research is concentrating on determining the factors that affect the selection of the growth pattern. [66]

The conclusion of the experiments done using electrodeposition to model growth is that the growth pattern depends directly on the anisotropy of the surface tension [2,3,4,22,59,63,70,75]. This crystalline anisotropy is necessary for dendrite formation. As the anisotropy decreases, the system becomes unstable. This instability causes the stable tips of the dendritic growth to split, causing the formation of a non-dendritic fractal. Dendrites are characterized by their complex, time-dependent side-branches and their stable tips, whereas non-dendritic fractals are characterized by tip-splitting. It is thought that crystalline anisotropy could be the mechanism that channels the growth of instabilities in certain preferred crystallographic directions. Or it could be that the anisotropy is the triggering mechanism for the needed instabilities. Without the anisotropy, the dendrite's growth would follow a crooked path rather than its normal straight path, leading to structures similar to non-dendritic fractals. [4]

The geometric model (GM) of Ben-Jacob et al. [2] shows that there is a critical level of anisotropy for a given driving force. Below this critical level, the interfacial dynamics of the dendrite is dominated by tip splitting. This is because the dendrite tip is unstable with respect to tip bifurcation. As the system is driven further from equilibrium (with anisotropy absent), the minimum length scale decreases and likewise the period between tip splittings decreases leading to the formation of a DLA structure.

An experiment performed by Sawada et al. [70] resulted in the realization of four growth regimes. The patterns were formed through the electrodeposition of zinc from a zinc sulfate solution. The growth regimes were defined by the electrolyte concentration, C, and the applied voltage, ΔV. At the lowest value of C (below 0.01 M) and low ΔV, (below about 8 V) the patterns were homogeneous, branching structures with a circularly symmetric outer boundary. As the concentration was reduced, the patterns became more and more like a non-dendritic fractal. At high C (about 0.1 M - 1 M) and low ΔV, the patterns were roughly fractal, but too thick for quantitative analysis. These deposits were open, branching and slow growing. At a high ΔV (above 8 V) and for a wide range of C values, the growth occurred quickly resulting in thin, stringy structures that were nonoriented. At intermediate values of C (about 0.03 - 0.1 M), dendrites were formed with well-defined "backbones" and single branches from the main stem at regular intervals. Even secondary and tertiary branches were observed. The boundary between these regimes is not definite. Sawada et al. [70] examined the importance of the velocity of growth in each of these regimes. When the electrolytic concentration was low, the velocity was independent of the applied voltage. At high concentrations, the velocity was strongly nonlinear with ΔV. In the latter case, the growth was slow and deposits that are roughly fractal were formed when ΔV was low. If ΔV was high, then fast growing, stringy patterns were formed. The growth velocity was linear in the voltage for the dendrite case. The transition from a disordered structure to a dendrite involved an increase in the growth speed. The homogeneous, tip-splitting structures became dendrites by two mechanisms, directly by an increase in the concentration and indirectly by an increase in growth velocity. Sawada et al. [70] calculated the fractal dimension for the homogeneous patterns formed. They found $D = 1.8 \pm 0.2$ at scales larger than a concentration dependent length δ. The fractal dimension for scales smaller than δ was 1.4 ± 0.2. The patterns were homogeneous above δ and fractal on scales below δ.

Another experiment with zinc leaves grown by electrodeposition, done by Matsushita et al. [47], examined the relationship between the fractal dimension of the growth patterns and the applied voltage. Their results showed that as the voltage was increased, while the concentration was kept constant, the

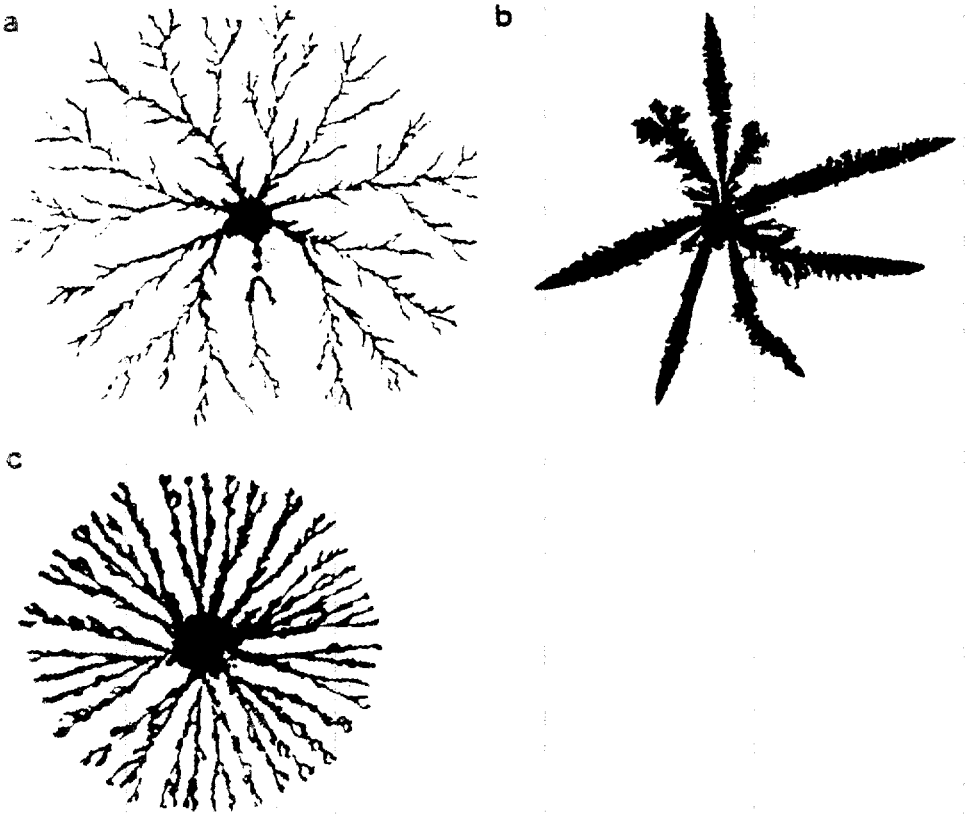

Figure 3:
a) Fractal growth of Zinc electrodeposits
b) Dendritic growth
c) Dense Radial Growth

fractal dimension increased. The experiment showed the existence of a threshold value of the voltage, which was about 8 V. Below this value, the fractal dimension is constant at around 1.66; above it, the fractal dimension increases linearly with the voltage. An experiment with zinc leaves done by Grier et al. [22], reaffirmed the findings of Matsushita et al., that there exists a threshold value of the voltage, above which, the fractal dimension increases. However, they measured a fractal dimension of 1.75 ± 0.03 for the highly branched fractal regime. Grier et al. also observed that the fractal dimension of the dendritic regime approached 1.0.

Another experiment done with electrodeposition by Sander [67] showed the existence of the third type of growth, the dense radial structure. The dense radial structures in the experiment of Grier et al. [23] are two-dimensional with rough branches that are contained in a circular envelope. These structures are not considered fractal because they fill the space uniformly, i.e. they are equally dense in every place. They are not considered dendrites because their tips are unstable. Dense radial structures are thought to form as a result of the combined effects of surface tension and a kinetic term in the boundary condition. These structures only develop when the diffusion length in a system is smaller than the radius of the cell that the structure is formed in [23]. Sander [67] observed that as the voltage and the concentration were increased, the structures changed from non-dendritic fractal to dense radial to dendritic. (See figure 4, reproduced from [67] with permission of the author.)

Nittman et al. [59] experimented to determine how the physical mechanisms that cause changes in anisotropy and the occurrence of tip splitting work. They used the Dielectric Breakdown Model (DBM) of Niemeyer et al. [57] on a triangular lattice. A seed is placed at the origin of a large circle of radius R. This seed represents the source of fluid with an infinitesimally small viscosity that is being forced, under pressure, to replace a fluid with higher viscosity. This interface moves according to Darcy's law: $v_n = -n \cdot \nabla P$ where v_n is the velocity component normal to the interface, n is the normal unit vector and P is the pressure field. P is constant in a less viscous fluid and in a more viscous fluid satisfies $\nabla^2 P = 0$ because $\nabla \cdot v = 0$. The boundary conditions that accompany this equation are: 1.) $P(r,\theta) = 1$ anywhere in the body with low viscosity and 2.) $P(R,\theta) = 0$ along the circle of radius R.

In a perfect medium, one that has radial symmetry and no pressure fluctuations, the interface would grow in concentric circles. When noise is added, instabilities occur causing irregularities in the interface. In the model of Nittman et al. [59], noise is introduced into the system by the random selection of the next perimeter site to be occupied, where the probability of going to each site depends on ∇P. The noise can be controlled by allowing the cluster to overtake a new perimeter site after it has been chosen s times, where s is a tunable parameter. As $s \to \infty$, the growth of the interface approaches the Darcy-law growth and each point grows according to the true local pressure gradient. When $s = 2$, the structure formed resembles the DBM structure both qualitatively and quantitatively, but with thicker branches. Its fractal dimension is 1.7.

When $s = 20$, the structure is still qualitatively different, but appears to cross to a new universality class with even thicker branches. However, the fractal dimension remains the same, 1.7. The fractal dimension is independent of the noise reduction and is always 1.7. The cluster grows smoothly, with no tip-splitting. As the radius of curvature increases, the interface becomes rough with positive (outward) and negative (inward) fluctuations. The positive fluctuations are insignificant, whereas, the negative fluctuations are important. The electric field in a single notch is small, which means that the notch is not filled in as quickly. (This is also because of the lack of interfacial tension.) The protrusions on each side of the notch have a larger electric field so they attract mass. This leads to the development of a fjord that is never filled in owing to the effect of screening.

If $s > 50$, the negative fluctuations decay more efficiently and the system is less susceptible to these fluctuations. As a result, a fjord is only formed at a large radius of curvature. The fractal dimension is independent of s, but W (the finger thickness) increases with s. Therefore, the larger s is, the smaller the amount of noise is, and the thicker the finger is. ($W = 4.5 \log s + 2$). W is independent of the magnitude of

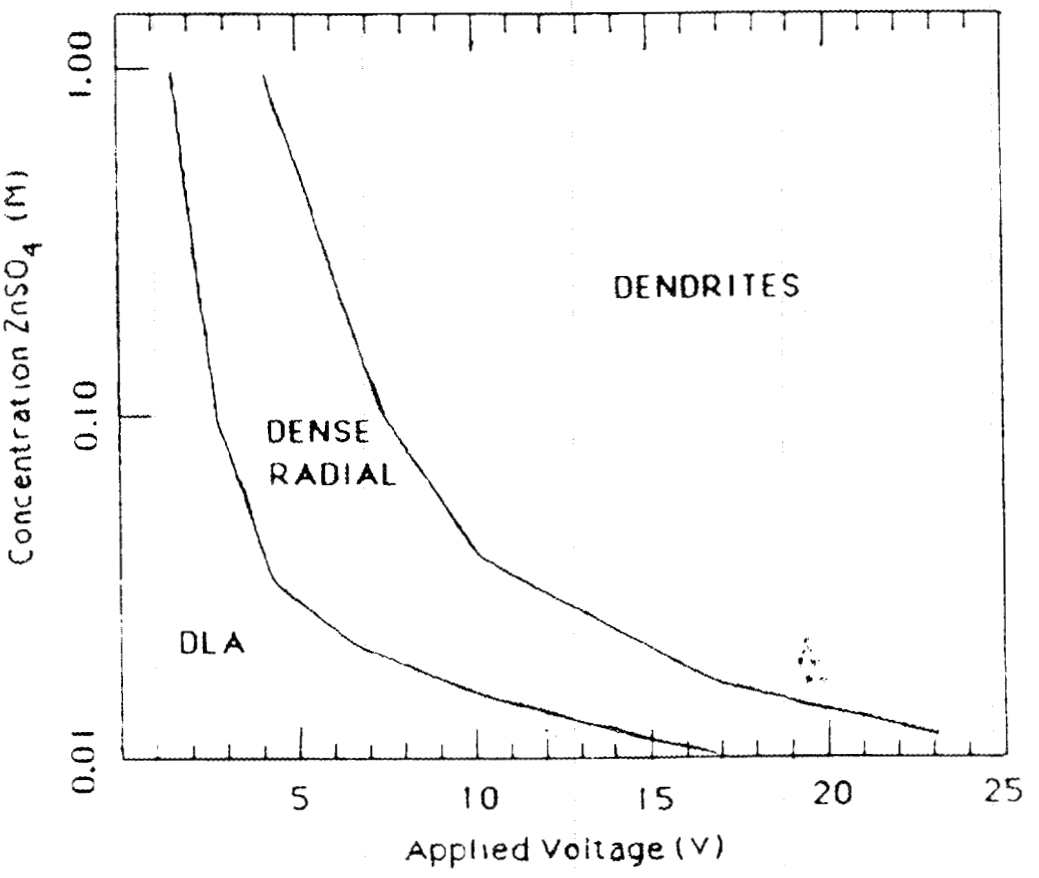

Figure 4: Observed regions of pattern formation in electrochemical deposition.

the pressure field. In this model, interfacial tension does not exist and the finger thickness is related solely to the amount of noise. Therefore, the tip-splitting is triggered by noise. The noise results in positive and negative fluctuations. Zero noise ($s = \infty$) leads to the formation of compact (non-fractal) circular objects. At a low noise level (large s), the noise has little effect when the cluster is small, but the effect is more pronounced as the cluster grows larger.

Real growth phenomena are never perfectly isotropic, and anisotropy seems to dominate dendritic crystal growth. Nittman et al. [59] modified their model to take into account anisotropy. Using the example of a snowflake, they realized that there are microscopic irregularities in the landing surface for the water molecules. So, they adjusted their model to take care of the fact that not all landing sites are created equal. The Darcy Law equation is replaced by $v_n = -n \cdot (k\nabla P)$. The conservation of mass condition, $\nabla \cdot v = 0$, implies that $\nabla \cdot (k\nabla P) = 0$ with the same boundary condition as for $k = 1$. $k = k(x,y)$ is the anisotropy parameter and represents the permeability in the fluid problem.

With $s = 50$ on a triangular lattice, varying the value of k showed that the structure formed looked more and more like a snowflake as k was increased. The structure has a fractal dimension of 1.5 ± 0.1. The individual branches on the object formed are disordered, with side branches of all sizes extending from it. The fractal dimension is greater than one because these side branches have many different length scales. These side branches look like a set of "trees" of varying height without branches. The height of the trees varies because of the screening effect. A tiny degree of anisotropy changes the fractal dimension of the object from the DLA value of 1.7 to 1.5 in the limit of infinite cluster size. The first of the equations given by Nittman et al. represents the growth law and relates the interfacial growth rate to the pressure field. The second equation describes the spatial changes in the pressure field that drives the instability.

CONCLUSION

Diffusion-limited solidification can lead to the formation of either dendrites or non-dendritic fractals, depending on the presence of crystalline anisotropy. The presence of anisotropy in a system causes the tips of the structure to remain stable, forming a dendrite. Isotropy causes the tips of the structure to split, forming a non-dendritic fractal. The future goal of research in this area is to determine what other factors, besides the presence of anisotropy, affect the selection of pattern growth.

Electrodeposition models of solidification lead to the formation of three types of growth patterns: dendrites, non-dendritic fractals, and dense radial structures. The question of which type is formed depends on the levels of voltage and concentration. When one or both of these are at a low level, non-dendritic fractals are formed. At intermediate levels, a crossover occurs and dense radial structures result. At high levels of both, dendrites are formed. A threshold level exists, above which the fractal dimension at a low concentration is no longer constant, but increases linearly with the voltage. It is probable that fractal geometry can be used to model dendritic growth because dendrites appear to be a special type of fractal. If fractal geometry can indeed be used to model dendritic growth, it will be yet another of the many applications of fractals to real phenomena.

BIBLIOGRAPHY

[1] Amar, M. Ben, Y. Pomeau, "Theory of Dendritic Growth in a Weakly Undercooled Melt," *Europhysics Letters*, **2** (No. 4), 307-314 (1986).

[2] Ben-Jacob, E., R. Godbey, Nigel D. Goldenfeld, J. Koplik, H. Levine, T. Mueller, L. M. Sander, "Experimental Demonstration of the Role of Anisotropy in Interfacial Pattern Formation," *Physical Review Letters*, **55** (No. 12), 1315-1318 (1985).

[3] Ben-Jacob, E., Nigel Goldenfeld, B. G. Kotliar, J. S. Langer, "Pattern Selection in Dendritic Solidification," *Physical Review Letters*, **53** (No. 22), 2110-2113 (1984).

[4] Ben-Jacob, E., Nigel Goldenfeld, J. S. Langer, Gerd Schön, "Dynamics of Interfacial Pattern Formation," *Physical Review Letters*, **51** (No. 21), 1930-1932 (1983).

[5] Ben-Jacob, E., Nigel Goldenfeld, J. S. Langer, Gerd Schön, "Boundary-Layer Model of Pattern Formation in Solidification," *Physical Review A*, **29** (No. 1), 330-340 (1984).

[6] Bolling, G. F., W. A. Tiller, "Growth From the Melt: III. Dendritic Growth," *Journal of Applied Physics*, **32** (No. 12), 2587-2605 (1961).

[7] Brady, R. M., R. C. Ball, "Fractal Growth of Copper Electrodeposits," *Nature*, **309** (No. 17), 225-229 (1984).

[8] Brower, Richard C., David A. Kessler, Joel Koplik, Herbert Levine, "Geometrical Approach to Moving-Interface Dynamics," *Physical Review Letters*, **51** (No. 13), 1111-1114 (1983).

[9] Brower, Richard C., David A. Kessler, Joel Koplik, Herbert Levine, "Geometrical Models of Interface Evolution," *Physical Review A*, **29** (No. 3), 1335-1342 (1984).

[10] Caroli, B., C. Caroli, B. Roulet, J. S. Langer, "Solvability Condition for Needle Crystals at Large Undercooling in a Nonlocal Model of Solidification," *Physical Review A*, **33** (No. 1), 442-452 (1986).

[11] Carslaw, H. S., J. C. Jaeger, *Conduction of Heat in Solids*, Oxford University Press, New York, 1984.

[12] Chalmers, Bruce, *Principles of Solidification*, John Wiley & Sons, Inc., New York, pp. 94-95 (1964).

[13] Dee, G., J. S. Langer, "Propagating Pattern Selection," *Physical Review Letters*, **50** (No. 6), 383-386 (1983).

[14] Dewdney, A. K., "Computer Recreations," *Scientific American*, **253** (No. 2), 16-24 (1985).

[15] Elam, W. T., S. A. Wolf, J. Sprague, D. U. Gubser, D. Van Vechten, G. L. Barz, Jr., Paul Meakin, "Fractal Aggregates in Sputter-Deposited $NbGe_2$ Films," *Physical Review Letters*, **54** (No. 7), 701-703 (1985).

[16] Feder, Jens, Torstein Jossang, "A Reversible Reaction Limiting Step in Irreversible Immunoglobulin Aggregation," *Scaling Phenomena in Disordered Systems*, edited by Roger Pynn and Arne Skjeltorp, NATO Advanced Study Institute Series, Series B, Physics, **133**, 99-131 (1985).

[17] Gardner, Martin, "Mathematical Games," *Scientific American*, **235** (No. 6), 124-128,133 (1977).

[18] Gefen, Yuval, Amnon Aharony, Benoit B. Mandelbrot, "Phase Transitions on Fractals: I. Quasi-linear Lattices," *Journal Physics A*, **16**, 1267-1278 (1983).

[19] Glicksman, M. E., R. J. Schaefer, "Investigation of Solid/Liquid Interface Temperatures Via Isenthalpic Solidification," *Journal of Crystal Growth*, **1**, 297-310 (1967).

[20] Glicksman, M. E., R. J. Schaefer, "Comments on Theoretical Analyses of Isenthalpic Solidification," *Journal of Crystal Growth*, **2**, 239-242 (1968).

[21] Glicksman, M. E., R. J. Schaefer, J. D. Ayers, "Dendritic Growth - A Test of Theory," *Metallurgical Transactions A*, **7A**, 1747-1759 (1976).

[22] Grier, D., E. Ben-Jacob, Roy Clarke, L. M. Sander, "Morphology and Microstructure in Electrochemical Deposition of Zinc," *Physical Review Letters*, **56** (No. 12), 1264-1267 (1986).

[23] Grier, David G., David A. Kessler, L. M. Sander, "Stability of the Dense Radial Morphology in Diffusive Pattern Formation," *Physical Review Letters*, **59** (No. 20), 2315-2318 (1987).

[24] Hong, D. C., J. S. Langer, "Analytic Theory of the Selection Mechanism in the Saffman-Taylor Problem," *Physical Review Letters*, **56** (No. 19), 2032-2035 (1986).

[25] Hultgren, Ralph, *Fundamentals of Physical Metallurgy*, Prentice-Hall, Inc., New York, 1952.

[26] Hutchinson, John E., "Fractals and Self Similarity," *Indiana University Mathematics Journal*, **30** (No. 5), 713-747 (1981).

[27] Kessler, David A., Joel Koplik, Herbert Levine, "Geometrical Models of Interface Evolution. II. Numerical Simulation," *Physical Review A*, **30** (No. 6), 3161-3174 (1984).

[28] Kessler, David A., Joel Koplik, Herbert Levine, "Dendritic Growth in a Channel," *Physical Review A*, **34** (No. 6), 4980-4987 (1986).

[29] Kessler, David A., Herbert Levine, "Stability of Dendritic Crystals," *Physical Review Letters*, **57** (No. 24), 3069-3072 (1986).

[30] Kessler, David A., Herbert Levine, "Theory of the Saffman-Taylor "Finger" Pattern. I," *Physical Review A*, **33** (No. 4), 2621-2633 (1986).

[31] Kessler, David A., Herbert Levine, "Theory of the Saffman-Taylor "Finger" Pattern. II," *Physical Review A*, **33** (No. 4), 2634-2639 (1986).

[32] Kolb, M., R. Botet, R. Jullien, "Scaling of Kinetically Growing Clusters," *Physical Review Letters*, **51** (No. 13), 1123-1126 (1983).

[33] Kolb, M., R. Jullien, R. Botet, "Scaling Properties of Cluster and Particle Aggregation," *Scaling Phenomena in Disordered Systems*, edited by Roger Pynn and Arne Skjeltorp, NATO Advanced Study Institute Series, Series B, Physics, **133**, 71-78 (1985).

[34] Kottler, G. R., W. A. Tiller, "Stability of the Needle Crystal," *Journal of Crystal Growth*, **2**, 287-307 (1968).

[35] Kuratowski, Kazimierz, Chapter 19 in *Introduction to Set Theory and Topology*, Addison-Wesley Publishing Co., Inc., Massachusetts, 1962.

[36] La Breque, Mort, "Fractal Symmetry," *Mosaic*, **16** (No. 1), 14-23 (1985).

[37] La Breque, Mort, "Fractal Applications," *Mosaic*, **17** (No. 4), 34-48 (1986).

[38] Langer, J. S., "Instabilities and Pattern Formation in Crystal Growth," *Reviews of Modern Physics*, **52** (No. 1), 1-28 (1980).

[39] Langer, J. S., "Existence of Needle Crystals in Local Models of Solidification," *Physical Review A*, **33** (No. 1), 435-441 (1986).

[40] Langer, J. S., H. Müller–Krumbhaar, "Theory of Dendritic Growth - I. Elements of a Stability Analysis," *Acta Metallurgica*, **26**, 1681-1687 (1978).

[41] Langer, J. S., H. Müller–Krumbhaar, "Theory of Dendritic Growth - II. Instabilities in the Limit of Vanishing Surface Tension," *Acta Metallurgica*, **26**, 1689-1695 (1978).

[42] Lee, Eui In, "Fractals for the PC," *PC Tech Journal*, November 1985, 165-178 (1985).

[43] Lindenmeyer, C. S., Bruce Chalmers, "Growth Rate of Ice Dendrites in Aqueous Solutions," *The Journal of Chemical Physics*, **45** (No. 8), 2807-2808 (1966).

[44] Liu, S. H., "Fractals and Their Applications in Condensed Matter Physics," *Solid State Physics*, **39**, 207-273 (1986).

[45] Mandelbrot, Benoit B., *The Fractal Geometry of Nature*, W. H. Freeman and Company, New York, 1983.

[46] Matsushita, M., Y. Hayakawa, S. Sato, K. Honda, "Scaling Properties for the Unscreened Surfaces of Fractal Patterns," *Physical Review Letters*, **59** (No. 1), 86-89 (1987).

[47] Matsushita, M., M. Sano, Y. Hayakawa, H. Honjo, Y. Sawada, "Fractal Structures of Zinc Metal Leaves Grown by Electrodeposition," *Physical Review Letters*, **53** (No. 3), 286-289 (1984).

[48] Meakin, Paul, "Diffusion-Controlled Cluster Formation in 2-6-Dimensional Space," *Physical Review A*, **27** (No. 3), 1495-1507 (1983).

[49] Meakin, Paul, "Diffusion-Controlled Formation in Two, Three, and Four Dimensions," *Physical Review A*, **27** (No. 1), 604-607 (1983).

[50] Meakin, Paul, "Formation of Fractal Clusters and Networks by Irreversible Diffusion-Limited Aggregation," *Physical Review Letters*, **51** (No. 13), 1119-1122 (1983).

[51] Müller–Krumbhaar, H., J. S. Langer, "Theory of Dendritic Growth - III. Effects of Surface Tension," *Acta Metallurgica*, **26**, 1697-1708 (1978).

[52] Müller–Krumbhaar, H., J. S. Langer, "Sidebranching Instabilities in a Two-Dimensional Model of Dendritic Solidification," *Acta Metallurgica*, **29**, 145-157 (1981).

[53] Mullins, W. W., R. F. Sekerka, "Morphological Stability of a Particle Growing by Diffusion or Heat Flow," *Journal of Applied Physics*, **34** (No. 2), 323-329 (1963).

[54] Nash, G. E., M. E. Glicksman, "Capillarity-Limited Steady-State Dendritic Growth - I. Theoretical Development," *Acta Metallurgica*, **22**, 1283-1290 (1974).

[55] Nash, G. E., M. E. Glicksman, "Capillarity-Limited Steady-State Dendritic Growth - II. Numerical Results," *Acta Metallurgica*, **22**, 1291-1299 (1974).

[56] Nauenberg, M., R. Richter, L. M. Sander, "Crossover in Diffusion-Limited Aggregation," *Physical Review B*, **28** (No. 3), 1649-1651 (1983).

[57] Niemeyer, L., L. Pietronero, H. J. Wiesmann, "Fractal Dimension of Dielectric Breakdown," *Physical Review Letters*, **52** (No. 12), 1033-1036 (1984).

[58] Nittman, Johann, Gerard Daccord, H. Eugene Stanley, "Fractal Growth of Viscous Fingers: Quantitative Characterization of a Fluid Instability Phenomenon," *Nature*, **314** (No. 14), 141-144 (1984).

[59] Nittmann, Johann, H. Eugene Stanley, "Tip Splitting Without Interfacial Tension and Dendritic Growth Patterns Arising From Molecular Anisotropy," *Nature*, **321** (No. 12), 663-668 (1986).

[60] Ohta, Shonosuke, Haruo Honjo, "Growth Probability Distribution in Irregular Fractal-like Crystal Growth of Ammonium Chloride," *Physical Review Letters*, **60** (No. 7), 611-614 (1988).

[61] Orbach, R., "Dynamics of Fractal Networks," *Science*, **231**, 814-819 (1986).

[62] Peitgen, H.-O., P. H. Richter, pp. 1-23 in *The Beauty of Fractals*, Springer-Verlag, New York, 1986.

[63] Radnoczi, Gy., T. Vicsek, L. M. Sander, D. Grier, "Growth of Fractal Crystals in Amorphous $GeSe_2$ Films," *Physical Review A*, **35** (No. 9), 4012-4015 (1987).

[64] Reed-Hill, Robert, *Physical Metallurgy Principles*, D. Van Nostrand Company, New York, 1973.

[65] Saito, Y., G. Goldbeck-Wood, H. Müller–Krumbhaar, "Dendritic Crystallization: Numerical Study of the One-Sided Model," *Physical Review Letters*, **58** (No. 15), 1541-1543 (1987).

[66] Sander, Leonard M., "Growth by Particle Aggregation," *Scaling Phenomena in Disordered Systems*, edited by Roger Pynn and Arne Skjeltorp, NATO Advanced Study Institute Series, Series B, Physics, **133**, 31-47 (1985).

[67] Sander, L. M., "Electrodeposition: Pattern Formation and Fractal Growth," *The Physics of Structure Formation*, **37**, 257-266 (1987).

[68] Sander, Leonard M., "Fractal Growth," *Scientific American*, **256** (No. 1), 94-100 (1987).

[69] Sander, L. M., P. Ramanlal, E. Ben-Jacob, "Diffusion-Limited Aggregation as a Deterministic Growth Process," *Physical Review A*, **32** (No. 5), 3160-3163 (1985).

[70] Sawada, Yasuji, A. Dougherty, J. P. Gollub, "Dendritic and Fractal Patterns in Electrolytic Metal Deposits," *Physical Review Letters*, **56** (No. 12), 1260-1263 (1986).

[71] Schroeder, Peter B., "Plotting the Mandelbrot Set," *Byte*, **11** (No. 13), 207-210 (1986).

[72] Sorensen, Peter R., "Fractals," *Byte*, **9** (No. 10), 157-172 (1984).

[73] Stanley, H. E., G. Daccord, H. J. Herrmann, J. Nittman, "Applications of Scaling and Disorderly Growth Phenomena to Oil Recovery," *Scaling Phenomena in Disordered Systems*, edited by Roger Pynn and Arne Skjeltorp, NATO Advanced Study Institute Series, Series B, Physics, **133**, 85-97 (1985).

[74] Stewart, Ian, "Les Fractals," *Mosaic*, **16** (No. 1), 10-13 (1985).

[75] Vicsek, Tamas, "Pattern Formation in Diffusion-Limited Aggregation," *Physical Review Letters*, **53** (No. 24), 2281-2284 (1984).

[76] Voss, Richard, "Random Fractal Forgeries: From Mountains to Music," *Science and Uncertainty*, Science Reviews Limited, pp. 69-85 (1985).

[77] Weitz, D. A. , M. Y. Lin, J. S. Huang, T. A. Witten, S. K. Sinha, J. S. Gethner, R. C. Ball, "Scaling in Colloid Aggregation," *Scaling Phenomena in Disordered Systems*, edited by Roger Pynn and Arne Skjeltorp, NATO Advanced Study Institute Series, Series B, Physics, **133**, 171-189 (1985).

[78] Wienberg, F., Bruce Chalmers, "Dendritic Growth in Lead," *Canadian Journal of Physics*, **29**, 382-392 (1951).

[79] Wienberg, F., Bruce Chalmers, "Further Observations on Dendritic Growth in Metals," *Canadian Journal of Physics*, **30**, 488-502 (1952).

[80] Witten, T. A., L. M. Sander, "Diffusion-Limited Aggregation, A Kinetic Critical Phenomenon," *Physical Review Letters*, **47** (No. 19), 1400-1403 (1981).

[81] Witten, T. A., L. M. Sander, "Diffusion-Limited Aggregation," *Physical Review B*, **27** (No. 9), 5686-5697 (1983).

[82] Wulff, John, Howard F. Taylor, Amos J. Shaler, *Metallurgy for Engineers*, John Wiley & Sons, Inc., New York, 1952.

INTERNAL DISTRIBUTION

1.	V. Alexiades	22.	J. M. Macdonald
2.	B. R. Appleton	23-27.	F. C. Maienschein
3.	L. C. Cain	28.	M. D. Morris
4.	C. S. Daw	29.	G. Ostrouchov
5.	J. B. Drake	30.	C. J. Remenyik
6.	Y. H. Etheridge	31-35.	L. A. Renker
7.	R. E. Flanery	36-40.	R. C. Ward
8.	G. A. Geist	41-45.	D. G. Wilson
9.	L. J. Gray	46.	P. H. Worley
10-11.	R. F. Harbison	47.	Central Research Library
12.	M. T. Heath	48.	K-25 Plant Library
13.	T. L. Hebble	49.	ORNL Patent Office
14.	T. Kaplan	50.	Y-12 Technical Library
15-19.	J. K. Ingersoll		/Document Reference Station
20.	S. M. Lenhart	51.	Laboratory Records - RC
21.	S. H. Liu	52-53.	Laboratory Records Department

EXTERNAL DISTRIBUTION

54. Dr. Donald M. Austin, ER-7, Applied Mathematical Sciences, Scientific Computing Staff, Office of Energy Research, Office G-437, Germantown, Washington, DC 20545

55. Dr. George I. Bell, T-7 Division, Los Alamos National Laboratory, P.O. Box 1663, Los Alamos, NM 87545

56. Dr. Bill L. Buzbee, C-3, Applications Support & Research, Los Alamos Scientific Laboratory, P. O. Box 1663, Los Alamos, NM 87545

57. Professor Alfredo Bermúdez de Castro, Universidad De Santiago, Dep. de Ecuaciones Funcionales, Facultad de Matematicas, Santiago de Compostela, SPAIN

58. Dr. Sam Coriell, U. S. National Bureau of Standards, Mathematical Analysis Section, Washington, DC 20234

59. Dr. James Corones, Ames Laboratory, Iowa State University, Ames, IA 50011

60. Dr. John J. Dorning, Department of Nuclear Engineering and Engineering Physics, Thornton Hall, University of Virginia, Charlottesville, VA 22901

61. Professor Antonio Fasano, Istituto Matematico Ulisse Dini, V. Le Morgagni 67/A, 50134 Firenze, ITALY

62. Professor Michael Fremond, Laboratoire Central des Pontes et Chaussees, Direction Scientific, 58 Boulevard Lefebvre, F-75732 Paris Cedex 15, FRANCE

63. Dr. Robert M. Haralick, Department of Electrical Engineering, University of Washington, Seattle, WA 98195

64. Professor Dr. Karl-Heinz Hoffman, Angewandte Mathematic I, Universität Augsburg, Memminger Strasse 6, D-8900 Augsburg, WEST GERMANY

65. Dr. Hans G. Kaper, Mathematics & Computer Science, Argonne National Laboratory, 9700 South Cass Avenue, Argonne, IL 60439

66. Dr. Robert J. Kee, Applied Mathematics Division, 8331, Sandia Laboratories, Livermore, CA 94550

67. Dr. W. Kurz, Laboratoire de metallurgie physique, Ecole polytechnique federale de Lausanne, Ch. de Bellerive 34-1007, Lausanne, SWITZERLAND

68. Dr. Alex Lehoczky, ES72 Space Science Laboratory, Marshall Space Flight Center, Huntsville, AL 35812

69. Dr. Richard A. Little, Mathematics and Computer Science Department, Baldwin-Wallace College, Berea, OH 44017

70. Dr. Basil Nichols, T-7, Mathematical Modeling and Analysis, Los Alamos Scientific Laboratory, P. O. Box 1663, Los Alamos, NM 87545

71. Professor Marek Niezgodka, Systems Research Institute, ul Newelska 6, 01-447 Warszawa, POLAND

72. Professor John R. Ockendon, Oxford University Computing Center, 24 St. Giles, Oxford OX1 3LB, UNITED KINGDOM

73. Dr. Ronald Peierls, Applied Mathematics Department, Brookhaven National Laboratory, Upton, NY 11973

74. Professor Mario Primiccerio, Inst. Matematico Ulisse Dini, Via Morgagni 67/A, I-50134 Firenze, ITALY

75. Dr. Timothy Riggle, Mathematics and Computer Science Department, Baldwin-Wallace College, Berea, OH 44017

76. Dr. Raoul Robert, Laboratoire I. M. A. G., B. P. No 68, 38402 Saint Martin d' Heres Cedex, FRANCE

77. Dr. Lawrence F. Shampine, Numerical Mathematics Division, 5642, Sandia Laboratories, P. O. Box 5800, Albuquerque, NM 87115

78. Professor Dr. Jürgen Sprekels, Angewandte Mathematic I, Universität Augsburg, Memminger Strasse 6, D-8900 Augsburg, WEST GERMANY

79. Dr. Don Steiner, Institute Professor, Department of Nuclear Engineering, Rensselaer Polytechnic Institute, Troy, NY 12181

80. Dr. Frank Szofran, ES72 Space Science Laboratory, Marshall Space Flight Center, Huntsville, AL 35812

81. Dr. Karl Hermann Tacke, Sonnerbergstrasse 7, 8134 Adliswil, SWITZERLAND

82. Professor Domingo Alberto Tarzia, Programme de Mathematical Pura y Applicada, Instituto de Matematica "Beppo Levi," Universidad Nacional de Rosario, Avenida Pelligrini 250, 2000 Rosario, ARGENTINA

83. Professor Rohit Trivedi, Ames Laboratory, Iowa State University, Ames, IA 50011

84. Professor Burton Wendroff, Mathematics Division, Los Alamos Scientific Laboratory, Los Alamos, NM 97544

85. Office of Assistant Manager for Energy Research and Development, U. S. Department of Energy, Oak Ridge Operations Office, Oak Ridge, TN 37830

86-95. Office of Scientific and Technical Information, P. O. Box 62, Oak Ridge, TN 37830